INTERNATIONAL JOURNAL FOR NUMERICAL METHODS IN ENGINEERING, VOL. 30, 1163–1179 (1990)

AN ELLIPTICAL GROWTH MODEL OF FOREST FIRE FRONTS AND ITS NUMERICAL SOLUTION

GWYNFOR D. RICHARDS

Department of Mathematics and Computer Science, Brandon University, Brandon, Manitoba, Canada R7A6A9

SUMMARY

A system of differential equations that describe the growth of a forest fire front in time for variable fuel, weather and topographical conditions is derived. The system is first order, non-linear and contains parameters that can be obtained from forestry data. A finite difference solution is presented, together with its inherent problems and their solution. Results are presented for a variety of situations that include variable fuel, wind and fire breaks. It is found that the equations and their solution efficiently produce simulations for complex problems.

INTRODUCTION

Millions of dollars each year are lost to forest fires in timber, communities and wildlife. Accurate prediction of forest fire behaviour is a valuable tool for the forest fire controller. A general model that can simulate forest fires would enable the prediction of the course of a fire in progress, so enabling more informed decisions concerning extinguishing strategies and evacuation of communities. It would also be useful in making predictions for a particular region for a variety of scenarios so that plans could be made ahead of time. The intuition of the forester is a valuable tool in fire fighting; this is gained in part from observing many actual fires. This process could be accelerated by using a fire simulator that used an accurate model. A contribution to the development of a computationally tractable general model of forest fire behaviour is the purpose of this paper.

Empirical data allow fairly accurate prediction of fire behaviour under constant conditions; however, the more probable situation involving such things as wind and fuel variations is a far more complex problem. Few workers have attacked this problem; the only computer simulations to date have been by Kourtz and co-workers,[1,2] Green[3] and Richards,[4] all based on cellular automata theory.[5] The properties of these techniques are not fully understood and in the author's opinion are not, as yet, developed to a stage of being a significant fire fighting tool. A great deal of interesting research remains to be done in this area.

The rate of spread and shape of a forest fire front is affected by a number of factors. The most important of these are:[6]

(i) fuel type and moisture content;
(ii) wind velocity and variability;
(iii) forest topography relative to the fire; fires spread faster up hill and cannot traverse natural barriers;

0029–5981/90/141163–17$08.50

Received April 1990

(iv) fuel continuity, i.e. is the fuel sparse or can it be considered to be homogeneous, also whether the fuel is of constant or variable type;
(v) the amount of spotting, i.e. burning material spread by the wind.

Extensive data have been collected from both natural and controlled fires with continuous uniform fuels involving constant wind velocity, moisture content and slope. The data indicate that under these conditions a fire ignited at a point reaches a quasi-steady state and progresses as a cigar shape that is biased toward the downwind direction and expands at a constant rate. The analytical approximation of the fire front most often used is that of an ellipse.[7,8] Other approximations that have been used include teardrops,[8] ovoids[9] and double ellipses.[10] Variations from elliptical behaviour are attributed to sparse fuels, spotting or variations from constant conditions. Recorded data has been curve fitted and incorporated into tables, slide-rules and other more complex prediction devices.[11] The curve fitted data cannot give predictions under variable conditions but are used extensively in the field as an aid to the intuition of the fire controller.

Anderson *et al.*[12] developed a graphical fire prediction method, based on Huygens' principle which assumes each point on the fire front at time t is the ignition point for a small fire that in a finite time interval dt burns out an elliptical region. Each ellipse is defined by the conditions at its generating point and dt, and the perimeter of the new fire front is defined by the envelope of all the ellipses. By successively drawing the ellipses and tracing out the new fire front the course of the fire can be plotted. Their results compared favourably with actual fires and the method is probably to date the most accurate predictor of fires under variable conditions.

In this work a system of differential equations is derived using the ideas of Anderson *et al.* but using infinitesimally small ellipses; their finite difference solution and its accompanying problems are also described. The equations can deal with variable weather and fuel conditions under the assumption that the eccentricity of the ellipses for a given fuel type is dependent on wind speed only. The performance of the model under a variety of complex conditions is illustrated.

THEORY

Under constant conditions for homogeneous, non-spotting fuels it is generally accepted that a fire ignited at a point will expand, at a constant rate, as an ellipse of the form[12]

$$\begin{aligned} x(s, t) &= at\cos s \\ y(s, t) &= bt\sin s \end{aligned} \tag{1}$$

where t is the time, the origin being the point of ignition and the y axis being the wind direction, Figure 1. The forward rate v, lateral rate u and the back rate w are defined as $b + c$, a and $b - c$ respectively. The Canadian Forest Fire Behaviour Prediction System (CFFBPS)[12] assumes elliptical growth and has documented values of u, v and w for a very large set of constant parameters affecting a fire. It has also been observed that, within certain limits, the ratio a/b is a function of wind speed only;[13] this is also an assumption of the CFFBPS.

The fire front at time t is represented parametrically in Cartesian co-ordinates by the closed curve $(x(s, t), y(s, t))$ where $0 \leqslant s \leqslant 2\pi$. It is assumed that each point on the fire front is an ignition point for a small fire that expands, igniting in time dt a small elliptical region around it. Taking θ to be the clockwise angle to the y axis defining the wind direction then the ellipse generated by a point $(x(s, t), y(s, t))$ is of the form, using local co-ordinates centred at $(x(s, t), y(s, t))$ and orientated at an angle θ to the original (x, y) axes, of equations (1) with $t = dt$, the parameters a, b and c being defined by the fuel, wind and topographical conditions at that point. dt is taken to

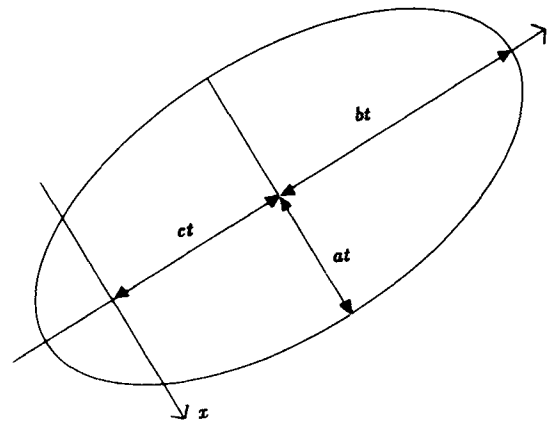

Figure 1. Fire front at time t for constant wind direction in the y direction

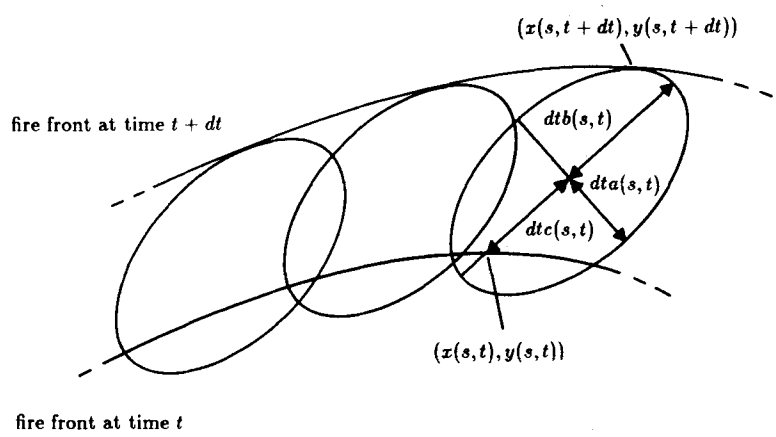

Figure 2. The envelope of ellipses forming the fire front at time $t + \mathrm{d}t$

be sufficiently small for a, b, c and θ to be assumed constant over that time period. The new fire front at time $t + \mathrm{d}t$ is now defined by the outer envelope of the ellipses generated at each point on the curve at time t. The tangential point of contact of the ellipse generated at $(x(s, t), y(s, t))$ with the envelope is defined as the point $(x(s, t + \mathrm{d}t), y(s, t + \mathrm{d}t))$, Figure 2.

The parameters a, b and c are taken to be functions of space and time, wind velocity is taken as a function of time only and the ratio a/b is taken to be a function of wind speed only. Since wind speed is a function of time only then so is a/b.

In the following analysis, given the curve $(x(s, t), y(s, t))$, $0 \leqslant s \leqslant 2\pi$, the curve $(x(s, t + \mathrm{d}t), y(s, t + \mathrm{d}t))$, $0 \leqslant s \leqslant 2\pi$, is derived for finite $\mathrm{d}t$. By limiting in $\mathrm{d}t$ the time derivatives $x_t(s, t)$ and $y_t(s, t)$ can be calculated. To calculate $(x(s, t + \mathrm{d}t), y(s, t + \mathrm{d}t))$ a linear transformation is applied that transforms the ellipses into circles. The equations of the envelope of circles can easily be calculated by a limiting process in $\mathrm{d}s$; $(x(s, t + \mathrm{d}t), y(s, t + \mathrm{d}t))$ is now obtained by applying the inverse of the linear transformation.

The axes are rotated so that the y direction is that of the wind; the x co-ordinate is then scaled by $b(s, t)/a(s, t)$, i.e. the following transformation is applied:

$$\begin{aligned} X &= [b(s, t)/a(s, t)](x\cos\theta - y\sin\theta) \\ Y &= x\sin\theta + y\cos\theta \end{aligned} \tag{2}$$

This transforms each of the ellipses to circles of radius $\mathrm{d}t\,b(s, t)$ with centres a distance $\mathrm{d}t\,c(s, t)$ above the point generating them. The envelope of ellipses is now an envelope of circles.

Figure 3 shows two such circles at time t at points s and $s + \mathrm{d}s$ on the transformed curve. The circle at $(s + \mathrm{d}s, t)$ has radius $\mathrm{d}t\,b(s + \mathrm{d}s, t)$ and its centre is a distance $\mathrm{d}t\,c(s + \mathrm{d}s, t)$ above the generating point; these values are shown as truncated Taylor series. The higher terms in $\mathrm{d}s$ are inferred and are eliminated in the preceding analysis when $\mathrm{d}s$ tends to zero.

The X co-ordinate of D is given by

$$\begin{aligned} X(s, t) + \mathrm{EF} &= X(s, t) + \mathrm{d}t\,b(s, t)\cos(\phi + \varphi - \varphi) \\ &= X(s, t) + \mathrm{d}t\,b(s, t)(\cos(\phi + \varphi)\cos\varphi + \sin(\phi + \varphi)\sin\varphi) \end{aligned} \tag{3}$$

The Y co-ordinate of D is given by

$$\begin{aligned} Y(s, t) + \mathrm{DE} + \mathrm{FG} &= Y(s, t) + \mathrm{d}t\,b(s, t)\sin(\phi + \varphi - \varphi) + \mathrm{d}t\,c(s, t) \\ &= Y(s, t) + \mathrm{d}t\,b(s, t)(\sin(\phi + \varphi)\cos\varphi - \sin\varphi\cos(\phi + \varphi)) + \mathrm{d}t\,c(s, t) \end{aligned} \tag{4}$$

Taking the cosines and sines from Figure 3 then

$$\begin{aligned} \cos(\phi + \varphi) &= \mathrm{AB}/\mathrm{AF} \\ \sin(\phi + \varphi) &= (\mathrm{AF}^2 - \mathrm{AB}^2)^{1/2}/\mathrm{AF} \\ \cos\varphi &= \mathrm{FI}/\mathrm{AF} \\ \sin\varphi &= (\mathrm{AF}^2 - \mathrm{FI}^2)^{1/2}/\mathrm{AF} \end{aligned}$$

where

$$\begin{aligned} \mathrm{AB} &= \mathrm{d}t\,\mathrm{d}s\,b_s(s, t) \\ \mathrm{AF} = (\mathrm{AI}^2 + \mathrm{FI}^2)^{1/2} &= \mathrm{d}s((\mathrm{d}t\,c_s(s, t) + Y_s(s, t))^2 + X_s^2(s, t))^{1/2} \\ \mathrm{FI} &= -\mathrm{d}s\,X_s(s, t) \end{aligned} \tag{5}$$

Since CD is tangential to both circles as $\mathrm{d}s$ tends to zero then C tends to D, CD tends to the tangent of the envelope and the co-ordinates of D tend to $(X(s, t + \mathrm{d}t), Y(s, t + \mathrm{d}t))$. Substituting equations (5) into (3) and (4) and letting $\mathrm{d}s$ tend to zero then

$$\begin{aligned} X(s, t + \mathrm{d}t) &= X(s, t) + \frac{\mathrm{d}t\,b(-X_s\,\mathrm{d}t\,b_s + (\mathrm{d}t\,c_s + Y_s)((\mathrm{d}t\,c_s + Y_s)^2 + X_s^2 - \mathrm{d}t^2 b_s^2)^{1/2})}{((\mathrm{d}t\,c_s + Y_s)^2 + X_s^2)} \\ &= X(s, t) + P(s, t, \mathrm{d}t) \end{aligned} \tag{6}$$

$$\begin{aligned} Y(s, t + \mathrm{d}t) &= Y(s, t) + \frac{\mathrm{d}t\,b(-((\mathrm{d}t\,c_s + Y_s)^2 + X_s^2 - \mathrm{d}t^2 b_s^2)^{1/2} X_s - (\mathrm{d}t\,c_s + Y_s)^2\,\mathrm{d}t\,b_s)}{((\mathrm{d}t\,c_s + Y_s)^2 + X_s^2)} + c\,\mathrm{d}t \\ &= Y(s, t) + Q(s, t, \mathrm{d}t) \end{aligned} \tag{7}$$

where all functions on the RHS are evaluated at (s, t). These are the equations of the envelope of circles formed in finite time $\mathrm{d}t$.

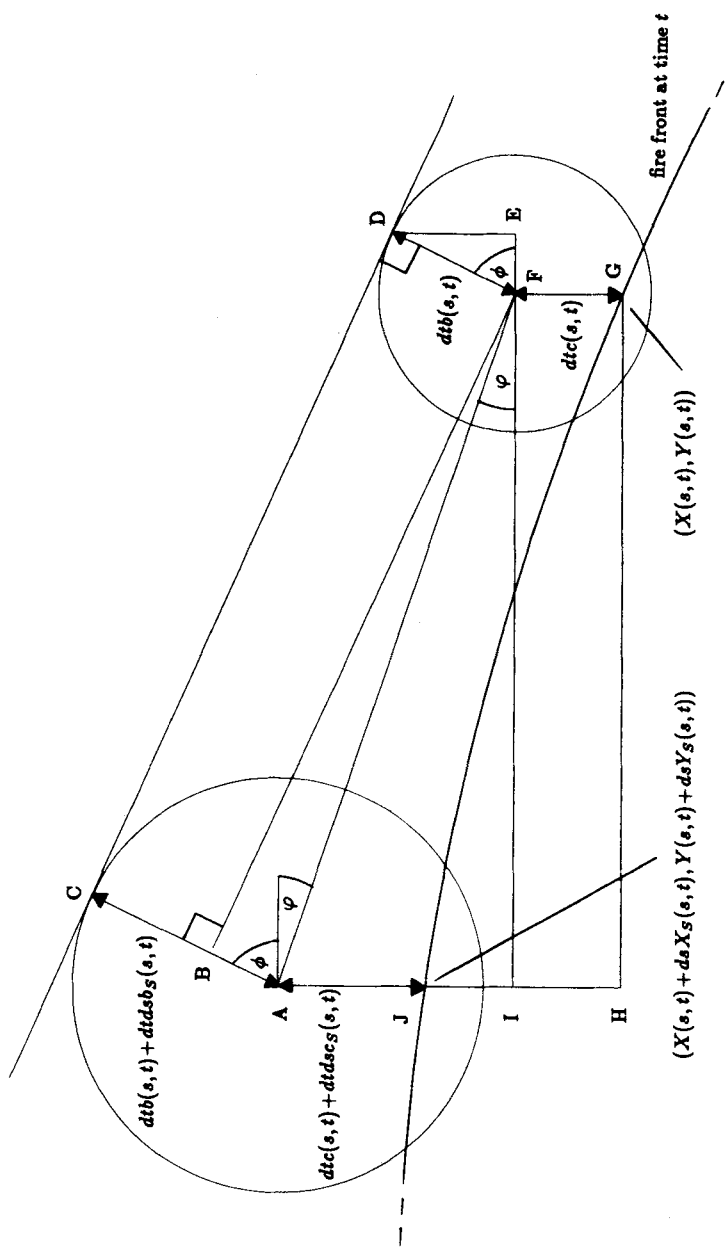

Figure 3. Circles at s and s + ds on the transformed fire front

The square root terms in equation (6) can become complex. When this happens radii of the circles on the curve are increasing so rapidly that the circle at (s, t) is completely surrounded by an adjacent one; hence an envelope is not formed. This problem can be avoided by making dt sufficiently small.

Transforming equations (6) and (7) back to (x, y) co-ordinates using the inverse of equations (2), i.e.

$$\begin{aligned} x &= [a(s,t)/b(s,t)]X\cos\theta + Y\sin\theta \\ y &= -[a(s,t)/b(s,t)]X\sin\theta + Y\cos\theta \end{aligned} \tag{8}$$

gives

$$\begin{aligned} x(s, t+dt) - x(s,t) &= [a(s,t)/b(s,t)]P(s,t,dt)\cos\theta + Q(s,t,dt)\sin\theta \\ y(s, t+dt) - y(s,t) &= -[a(s,t)/b(s,t)]P(s,t,dt)\sin\theta + Q(s,t,dt)\cos\theta \end{aligned} \tag{9}$$

By dividing both sides of equations (9) and (10) by dt, substituting for X and Y into P and Q using equations (2) and letting dt tend to zero, then the time derivatives $x_t(s, t)$ and $y_t(s, t)$ are obtained, i.e. after rearranging

$$x_t = \frac{a^2\cos\theta(x_s\sin\theta + y_s\cos\theta) - b^2\sin\theta(x_s\cos\theta - y_s\sin\theta)}{(b^2(x_s\cos\theta - y_s\sin\theta)^2 + a^2(x_s\sin\theta + y_s\cos\theta)^2)^{1/2}} + c\sin\theta \tag{10}$$

$$y_t = \frac{-a^2\sin\theta(x_s\sin\theta + y_s\cos\theta) - b^2\cos\theta(x_s\cos\theta - y_s\sin\theta)}{(b^2(x_s\cos\theta - y_s\sin\theta)^2 + a^2(x_s\sin\theta + y_s\cos\theta)^2)^{1/2}} + c\cos\theta \tag{11}$$

These are the equations of fire front growth based on growth by envelopes of infinitesimally small ellipses, subject to the initial conditions

$$\begin{aligned} x(s, 0) &= x_0(s) \\ y(s, 0) &= y_0(s) \end{aligned} \tag{12}$$

If a, b, c and θ are constant, then for a fire ignited at a point source, the equations, to be consistent with the model, should predict a constantly expanding ellipse of the form of equations (1). Setting θ to zero and approximating a point ignition source as a small ellipse of the form

$$\begin{aligned} x_0(s) &= a\,dt\cos s \\ y_0(s) &= b\,dt\sin s + c\,dt \end{aligned} \tag{13}$$

then it is found that the ellipse

$$\begin{aligned} x(s, t) &= a(t + dt)\cos s \\ y(s, t) &= b(t + dt)\sin s + c(t + dt) \end{aligned} \tag{14}$$

satisfies equations (11) and (12), i.e. the equations are consistent with the model, regardless of how small dt is. This is also the case for any angle θ.

It is possible for the curve to cross over itself; this may occur at concave points and when two separate regions of the curve meet. Around a sufficiently concave region of the curve, the regions either side continuously burn in front of it so that it does not contribute to the front at a later time. This causes an internal loop to form that grows into the interior of the curve. When two separate regions of the curve meet an internal unburnt area is formed that eventually burns itself out. Figure 4 shows these two effects schematically at time t, before cross-over, and time $t + dt$,

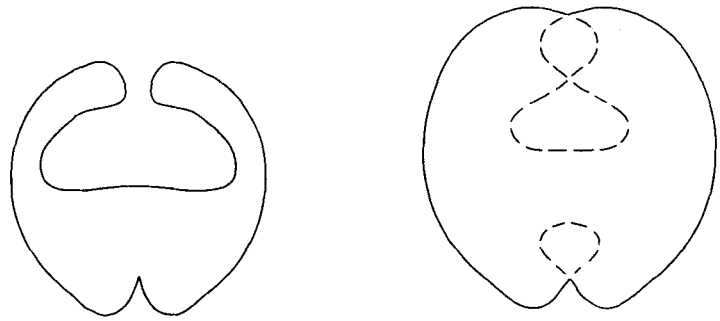

Figure 4. The formation of internal loops by a concave point and by two separate regions crossing

after cross-over, as the solid and dashed line. Since the main interest is the outer fire front, at time $t + dt$ the fire front is taken to be the outer portion of the curve, i.e. the solid curve.

The important features of these equations are: firstly they are a system of first order differential equations which, although intractable analytically, are easily solved numerically; secondly the parameters a, b and c for a fire can be obtained from the CFFBPS, and thirdly they can model fires involving variable fuel and wind.

NUMERICAL ANALYSIS AND RESULTS

Method of solution

The curve $(x(s, t), y(s, t))$ is discretized into $n + 1$ points $(x_{i,j}, y_{i,j})$ such that

$$(x_{i,j}, y_{i,j}) = (x(i\,ds, j\,dt),\ y(i\,ds, j\,dt)) \tag{15}$$

where $ds = 2\pi/n$, ds and dt are the parameter and time step sizes and $(x_{0,j}, y_{0,j}) = (x_{n,j}, y_{n,j})$.

Given $(x_{i,j}, y_{i,j})$ then $(x_{i,j+1}, y_{i,j+1})$ is approximated using the modified Euler's method with one correcting iteration. Since a, b and c are functions of s and t the RHS of equations (10) and (11) can be written in the form

$$\begin{aligned} x_t &= F(s, t, x_s, y_s) \\ y_t &= G(s, t, x_s, y_s) \end{aligned} \tag{16}$$

Using central difference approximations for the derivatives x_s and y_s, the numerical method becomes

Predictor

$$\begin{aligned} dx_{i,j} &= dtF(i\,ds, j\,dt, (x_{i+1,j} - x_{i-1,j})/2\,ds, (y_{i+1,j} - y_{i-1,j})/2\,ds) \\ \bar{x}_{i,j+1} &= x_{i,j} + dx_{i,j} \end{aligned} \tag{17}$$

with similar expressions for $dy_{i,j}$ and $\bar{y}_{i,j+1}$.

Corrector

$$\overline{dx}_{i,j} = dtF(i\,ds, (j+1)\,dt, (\bar{x}_{i+1,j+1} - \bar{x}_{i-1,j+1})/2\,ds, (\bar{y}_{i+1,j+1} - \bar{y}_{i-1,j+1})/2ds) \tag{18}$$

and similarly for $\overline{dy}_{i,j}$. Then

$$x_{i,j+1} = x_{i,j} + 0{\cdot}5(dx_{i,j} + \overline{dx}_{i,j})$$
$$y_{i,j+1} = y_{i,j} + 0{\cdot}5(dy_{i,j} + \overline{dy}_{i,j}) \tag{19}$$

For fires ignited at a point source the initial curve is taken to be a very small ellipse. The initial conditions for point source ignition are, where a, b and c are evaluated at the ignition point,

$$x_{i,0} = dt a \cos i ds$$
$$y_{i,0} = dt b \sin i ds + dt c \tag{20}$$

Although more sophisticated numerical methods that allow larger time steps could have been used it was found that this method was adequate, as small time steps were required to avoid jumping over fire breaks and the formation of excessively large loops at concave regions.

For the simulations in this paper the point source ignition was given by equations (19) using 200 points on the curve; dt was 50 s. Reductions of dt or increasing the number of points on the curve produced little or no change in the results. The C.P.U. times for the simulations on a VAX 8700 are given to the nearest second.

Wind changes over uniform fuel

If a, b and c are time dependent only and the initial curve is convex then the curve remains convex and hence does not cross over itself. If this is the case then the solution of the problem is a straightforward application of equations (17) and (18). An important, commonly occurring example of such fires occurs when all the factors affecting a fire are constant apart from the wind velocity.

Figure 5 illustrates the effects of three successive wind changes on a forest fire. The contours are the points on the curve joined by straight lines, the cross is the ignition point. The fronts are shown at 1500 s and intervals of 1000 s thereafter; dt was 50 s. Wind speed is increased by increasing a, b and c and wind direction is changed by changing θ. θ was initially zero and changed to $-\pi/4$, 0 and $\pi/8$ at 2500, 3500 and 5500 s respectively. a, b and c were initially 0·02, 0·04 and 0·03 m s^{-1} respectively and then changed to 0·02, 0·06 and 0·05 m s^{-1} at 3500 s; these values are equivalent to wind speeds of 25 and 30 km/h over red and white pine of medium moisture content. Increasing wind speed increases the rate of spread and changing wind direction changes the fastest burning portions of the curve to those with outward normals closest to the wind direction. Changing wind direction also destroys the symmetry of the curve. The time for the simulation was 3 s, suggesting that this type of problem could easily be transferred to a micro computer.

Wind direction is rarely exactly unidirectional; a distribution about a mean is more likely. A question that has not yet been fully answered is the effect of such wind variations. Figure 6 illustrates the fire fronts for constant wind speed but with random variations of θ. At each time step a random number generator was used to choose θ between $-\pi/4$ and $\pi/4$. After a sufficient number of iterations the fronts settle down to oval-like shapes, symmetric in both axes of length to breadth ratio 1·8:1. If the wind direction were constant the length to breadth ratio would be 3:1. The values of a, b and c are equivalent to a 30 km/h wind over mature jack pine of medium moisture content. The fronts are shown at 500 s and at intervals of 1000 s thereafter. The distance from the ignition point to the tip of the final contour was 500 m. The time for the simulation was 8 s. The time for this simulation was longer then the previous one as a regriding process that

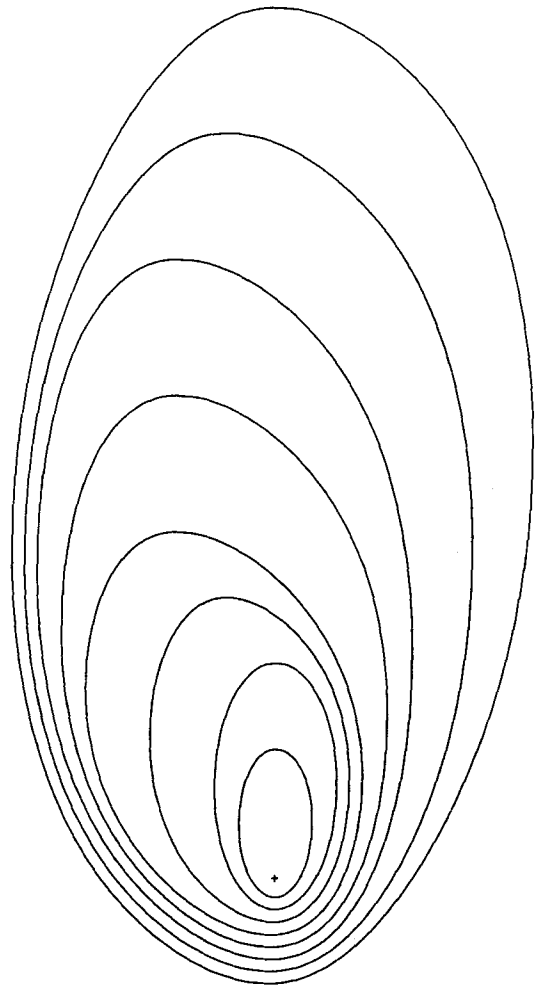

Figure 5. The effect of wind velocity changes over uniform fuel

added more points to the curve was used; this process is described in the following section. The final curve contained 250 points. This model enables tables of fire fronts for different wind velocity distributions to be made for particular fuels.

Regriding

Regriding (i.e. rediscretization of the curve) is required when the density of points on a part of the curve becomes sparse. If the number of points remains constant as the curve grows then distances between points increase, especially in fast moving regions. Large distances between points introduce errors into the approximations of x_s and y_s, and hence into the whole simulation.

Another, and dramatic, example of large distances forming between points occurs when a fire spreads around a fire break, Figure 7. The fronts are shown at 1500 s and intervals of 1000 s thereafter; this is the case for all the following figures as well. The values of a, b and c are equivalent to a 30 km/h wind over mature jack pine of medium moisture content. The break is an

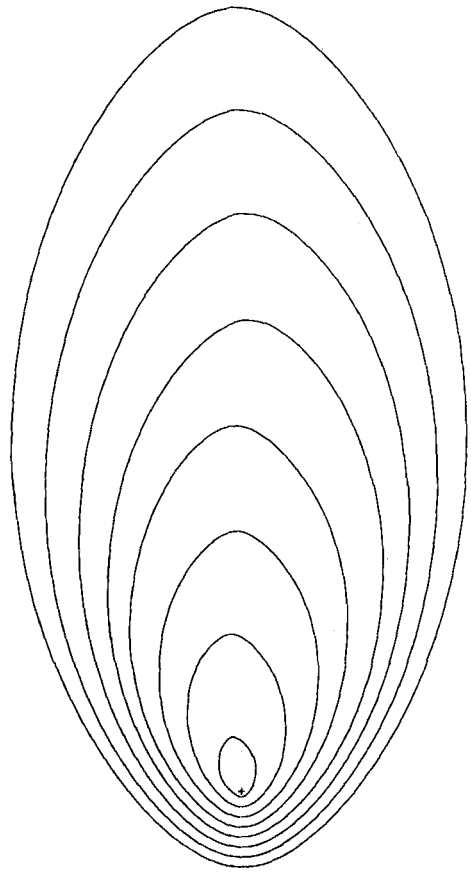

Figure 6. The effect of random wind directions between $-\pi/4$ and $\pi/4$ over uniform fuel; $a = 0{\cdot}02\ \mathrm{m\,s^{-1}}$, $b = 0{\cdot}04\ \mathrm{m\,s^{-1}}$, $c = 0{\cdot}03\ \mathrm{m\,s^{-1}}$, $dt = 50\ \mathrm{s}$, $t = 5\ \mathrm{m}$

area 80 m long where a, b and c are set to zero. As points enter the break they remain there, the oscillatory line at the base of the break being caused by such points. Eventually at either end of the break there are two consecutive points such that one is inside the break, and one outside that does not enter the break. The point outside continually moves downwind, the other remains stationary. The inadequacy of the simulation is obvious.

When distributing points around the curve the highest density of points should be in areas of high curvature. There are many ways of doing this; the following technique was found to be a balance between effectiveness and efficiency. Figure 8 shows the line segment joining points at $i = k$ and $k - 1$ of length l_k, with the two adjoining segments before and after regriding. θ_k is the acute angle between line segments at k. The following test is applied to each pair of points on the curve in order. If

$$\max(\cos(\theta_k/2), \cos(\theta_{k-1}/2)) > (T/l_k)^2 \tag{21}$$

where T is a specified threshold, then an extra point is added at the midpoint of the line segment. This process is now repeated recursively to both halves of the segment until the condition is satisfied by all new points between k and $k - 1$. All points after $k - 1$ are now assigned new values of i. The closer θ_k and θ_{k-1} are to π (i.e. the closer the line segments are to being collinear) then the

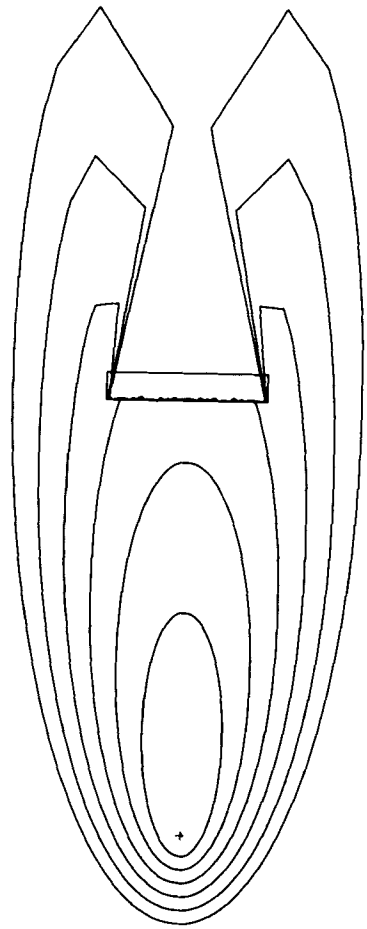

Figure 7. Fire fronts around a fire break without regriding; $a = 0{\cdot}02\ \mathrm{m\,s^{-1}}$, $b = 0{\cdot}06\ \mathrm{m\,s^{-1}}$, $c = 0{\cdot}05\ \mathrm{m\,s^{-1}}$, $\mathrm{d}t = 50\ \mathrm{s}$

larger the allowable value of l_k. This ensures a high density of points in areas of high curvature without placing unnecessary points in areas of low curvature. Raising the power of T/l_k biases the regriding even more to the areas of high curvature; taking the square was found to be effective.

Figure 9 shows the effectiveness of regriding applied to the previous fire break problem, with $T = 1$ m. Although regriding was applied at each time step it did not add any new points until the 3rd shown contour, i.e. till areas of high curvature were formed when the fire began to curl around the break. The final front had 330 points and the total time for the simulation was 6 s.

Clipping

As mentioned before, around concave regions the curve can cross over itself, forming a loop that spreads into the interior of the curve. We are interested in the external curve only. If the loop is not removed regriding will add a large number of redundant points, as in its initial stages its curvature is very high. Also, as will be discussed later, in areas where the derivatives of a, b and c in s are high, the number of points contained in such loops can grow exponentially, so rendering the simulation useless. The removal of such loops is called loop clipping.

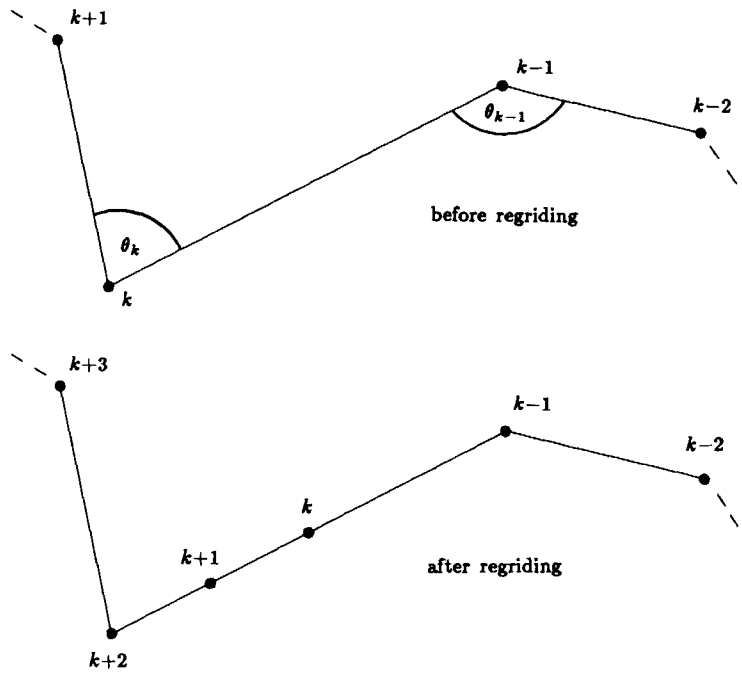

Figure 8. The introduction, by regriding, of new points on the line joining points at k and $k-1$ and the renumbering of subsequent points

Cross-over can occur when two entirely separate parts of the curve intersect, forming a possibly very large, internal loop that crosses over itself at least once. An example can be seen in the previous fire break problem where the two arms on either side of the break will eventually meet. The removal of such loops is called cross-over clipping.

Figure 10 shows, schematically, a portion of the curve at time t around a concave point at $i = k$, the formation of a loop at $t + \mathrm{d}t$ and the loop clipped. The loop clipping process at $t + \mathrm{d}t$ involves identifying the point of intersection of the loop with the external curve, the addition of a new discretizing point at the intersection and finally reassigning new values of i to the points on the clipped curve. The concave point k at time t will always be part of the loop at $t + \mathrm{d}t$ if one is formed.

At each time step the curve is searched for concave points. If any loops are formed at the next time step it is known that their intersection with the external curve must be either side of points that were concave at the previous time step. By testing for the intersection of line segments either side of such points k, the point of intersection with the external curve can be found. If a loop crosses over itself, the required point of intersection is that between intersecting line segments furthest apart on the curve. The search process need only be performed a small distance either side of k to ensure identification of the intersection point. The required distance either side of k is dependent on the $\mathrm{d}t$ (the larger $\mathrm{d}t$ the larger the loop), and the density of the points on the curve (which is dependent on the regriding threshold T). For the values of $\mathrm{d}t$ and T used here, searching 15 points either side of concave points removed all internal loops.

For cross-over clipping the process is the same except that the identification of the intersection of the internal loop with the external curve is not easy, as there is no simple way of predicting when and where it will occur. The point of intersection can be identified interactively or by

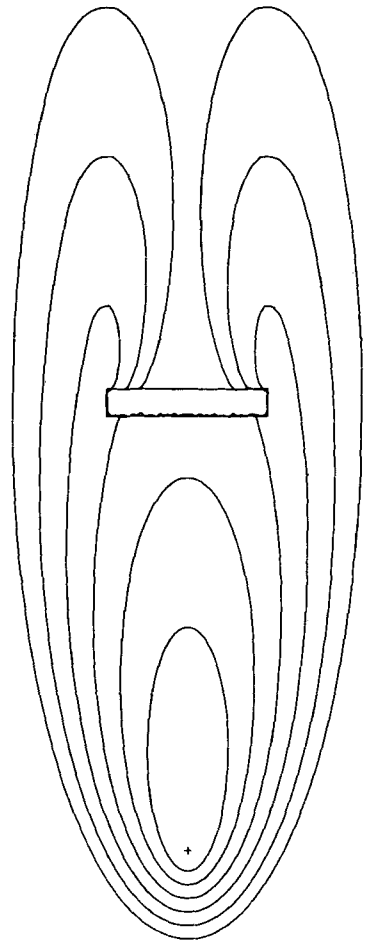

Figure 9. Fire fronts around a fire break with regriding; $a = 0{\cdot}02\ \mathrm{m\,s^{-1}}$, $b = 0{\cdot}06\ \mathrm{m\,s^{-1}}$, $c = 0{\cdot}05\ \mathrm{m\,s^{-1}}$, $\mathrm{d}t = 50\ \mathrm{s}$, $T = 1\ \mathrm{m}$

periodically testing for the intersection of every line segment with every other line segment. If segments are found to have intersected then an internal loop has been formed, with its intersection with the external curve being the intersection of line segments furthest apart on the curve.

The complete algorithm

Given the points $(x_{i,j}, y_{i,j})$ on the curve the full algorithm becomes

1. Identify concave points.
2. Approximate curve at next time step.
3. Perform loop clipping around previously concave points.
4. Perform cross-over clipping if cross-over has been identified.
5. Perform regriding so as to finally obtain the points $(x_{i,j+1}, y_{i,j+1})$.

The algorithm, although fairly technical, can be written in about 300–400 lines in a high level language.

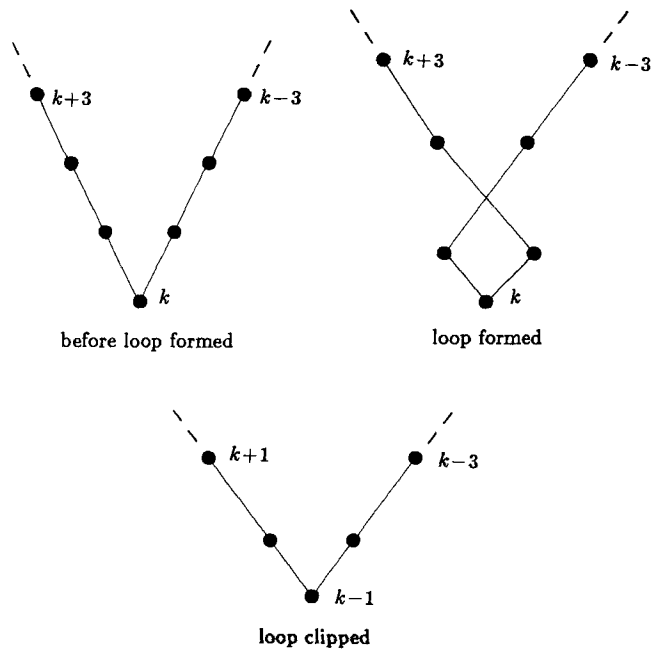

Figure 10. The formation of loop at a concave point, its removal, the insertion of a new discretizing point and the renumbering of subsequent points

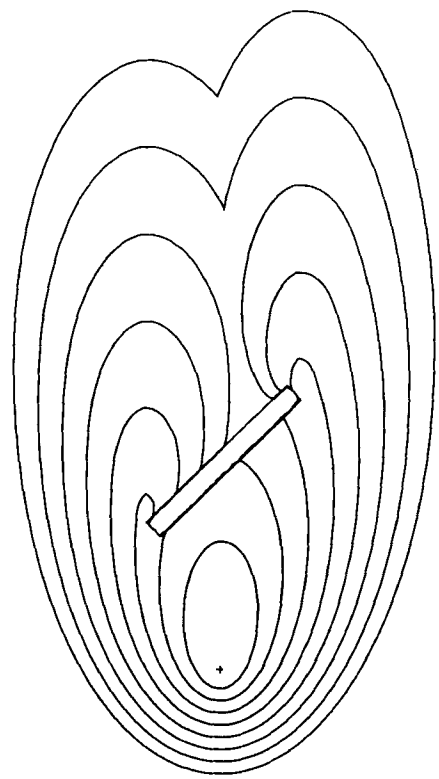

Figure 11. Two separate regions of a fire front either side of a fire break crossing over forming an internal loop that is clipped, forming a concave point; $a = 0{\cdot}02\ \mathrm{m\,s^{-1}}$, $b = 0{\cdot}04\ \mathrm{m\,s^{-1}}$, $c = 0{\cdot}03\ \mathrm{m\,s^{-1}}$, $dt = 50\ \mathrm{s}$, $T = 0{\cdot}8\ \mathrm{m}$

The fire break problem of Figure 11 shows all aspects of the algorithm in operation. Regriding was applied at each time step. The break is 90 m long and the values of a, b and c are equivalent to 25 km/h wind over mature jack pine of medium moisture content. As the curve curls around the break the number of points increases steadily owing to regriding. Cross-over was identified, interactively, a little before 6500 s, at which point the internal loop was clipped. In performing cross-over clipping a concave point is formed; loop clipping is performed at every time step thereafter. A loop was identified at every time step; however, if the simulation is allowed to continue the concave point becomes less severe and loops occur less frequently. If the loop is not removed it will spread back towards the fire break, creating a large number of redundant extra points.

After cross-over clipping the number of points drops from 370 to 209 as the large number of points at the fire break are removed. The final front has 214 points. Technically there is an internal unburnt area that eventually burns itself out; however, the main interest is the outer fire front not the internal one (unless you are in the middle of it !). The total time for simulation was 11 s.

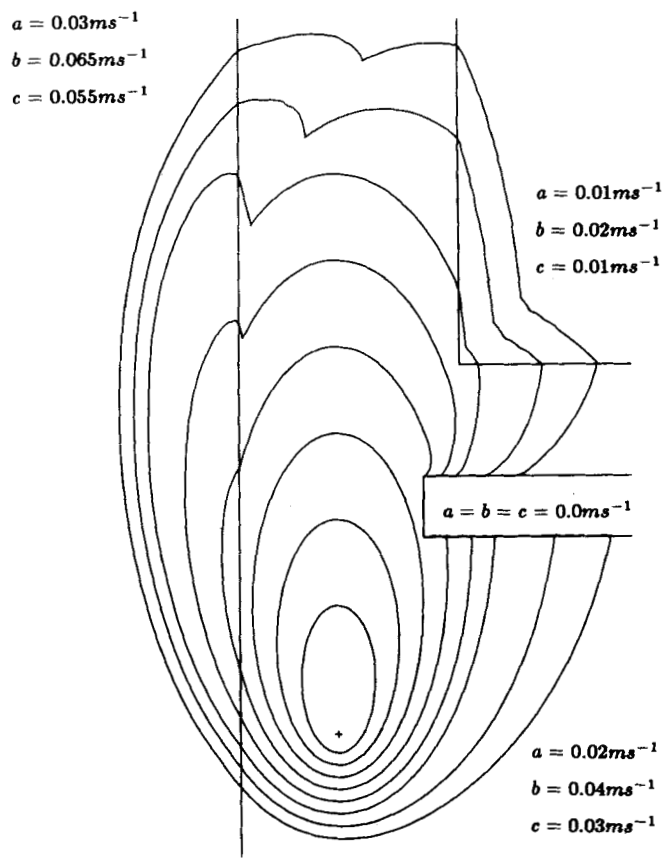

Figure 12. Fire fronts over 4 different fuel types with a wind direction change; dt = 50 s, T = 1 m

Variable wind and fuel

Figure 12, the final example, shows the performance of the simulation in dealing with four different fuel types and a wind change, the fire break being 30 m wide. The values of a, b and c for the left, central and top right regions are equivalent to spruce lichen woodland of medium, high and very high moisture content respectively, with a wind speed of 25 km/h. The fire expands elliptically from the point of ignition in the central region until it reaches the faster burning left hand region. The rate of spread up the left hand side of the fuel interface tends to the forward rate of the left hand region. As the fire spreads up the left hand side of the interface it ignites the right hand side which then burns into the central region.

On the other side of the fuel bed the fire meets the fire break and burns along its edges, the change in wind direction closer to that of the edges of the break increasing the rate of spread along the break. The rates on both sides tend to the same constant rate. In meeting the slow burning top right region the fire slows down. The wind direction was changed to $\pi/4$ at 5500 s, i.e. just after the second but last shown contour. The time for the simulation was 37 s and the final front had 320 points.

In crossing a fuel interface concave points are formed which then form loops. If a loop is not clipped it will grow and cross the interface and, in general, form two concave points that will form loops that will in turn cross the interface, each forming two more concave points, etc. The regriding process will add points to these loops and the number of points increases so rapidly that without loop clipping the simulation grinds to a halt.

CONCLUSIONS

A system of differential equations based on elliptical fire growth has been derived for a forest fire front represented as a closed curve. The equations are a relatively simple first order non-linear system with parameters directly available from forestry data. The equations allow for time-dependent wind velocity and spatially variable fuel type.

In solving the system a simple predictor/corrector method was found to be effective although rediscretization of the curve was required to ensure a sufficient density of points in all regions of the curve. For problems where the curve does not cross over itself, such as the important uniform fuel, variable wind velocity problem, solutions were obtained in a matter of seconds, suggesting that the model could be transferred to a micro computer for use in the field. For problems where the curve crosses over itself a clipping procedure was introduced; this increased the time of the simulation, though problems involving variable fuel types and wind velocity changes were still solved very quickly. Although based on known results concerning forest fire behaviour, the accuracy of the model can be verified only by comparison with actual fires and polling fire fighters as to whether the accuracy is sufficiently good to be of use to them.

In conclusion, this technique is based on principles already in use by fire fighters and can efficiently solve hitherto unsolved problems. The model is not entirely general but hopefully is a significant contribution to such a theory.

ACKNOWLEDGEMENTS

The author would like to thank Dr G. M. Richards for her invaluable help and encouragement. Thanks are also due to Prof. P. Townsend and the staff of the Department of Mathematics and Computer Science at Swansea University for providing an atmosphere conducive for research during his sabbatical leave there.

REFERENCES

1. P. Kourtz, S. Nozaki and W. O'Reagan, 'Forest fires in the computer—A model to predict the perimeter and location of a forest fire', Canadian Forestry Service, *Information Report FF-x-65*, 1977.
2. P. Kourtz and W. G. O'Reagan, 'A model for a small forest fire . . . to simulate burned and burning areas for use in a detection model', *Forest Sci.*, **17**(2), 163–169 (1971).
3. D. G. Green, 'Shapes of fires in discrete fuels', *Ecological Modelling*, **20,** 21–32 (1983).
4. G. D. Richards, 'Numerical simulation of forest fires,' *Int. j. numer. methods eng.*, **25,** 625–634 (1988).
5. S. Wolfram, 'Cellular automata as a model of complexity', *Nature*, **311,** 419–424 (1984).
6. W. Fons, 'Analysis of fire spread in light forest fuels', *J. Agr. Res.*, **72**(3), 93–121 (1946).
7. D. G. Green, A. M. Gill and I. R. Noble, 'Fire shapes and the adequacy of spread models', *Ecological Modelling*, **20,** 33–45 (1983).
8. C. E. Van Wagner, 'A simple fire growth model', *Forestry Chron.*, **45,** 103–104 (1969).
9. G. B. Peet, 'The shape of mild fires in jeera forest', *Aus. Forestry*, **31,** 121–127 (1967).
10. F. A. Albini, 'Estimating wildfire behaviour and effects', *USDA For. Gen. Technical Report INT-30*, 1976.
11. B. D. Lawson, B. J. Stocks, M. E. Alexander and C. E. Van Wagner, 'A system for predicting fire behaviour in Canadian forests', *on Proc 8th Natl. Conf. on Fire and Forest Meteorology*, Society of American Foresters, Washington, D.C., 1985.
12. D. H. Anderson, E. A. Catchpole, N. J. DeMestre and T. Parkes, 'Modelling the spread of grassland fires', *J. Austral. Math. Soc. (Series B)*, **13,** 452–466 (1982).
13. M. E. Alexander, 'Estimating the length-to-breadth ratio of elliptical forest fire patterns', *Proc 8th Natl. Conf. on Fire and Forest Meteorology*, Society of American Foresters, Washington, D.C., 1985.